

TRITIUM TRANSPORT IN POLOIDAL FLOWS OF A DCLL BLANKET

M.J. Pattison¹, S. Smolentsev², R. Munipalli¹, M.A. Abdou²

¹HyPerComp Inc., Westlake Village, CA 91361, mjp@hypercomp.net

²MAE Department, University of California, Los Angeles, CA 90095, sergey@fusion.ucla.edu

In a Dual-Coolant Lead-Lithium (DCLL) blanket, tritium losses from the PbLi into cooling helium streams may occur when the liquid-metal breeder is moving in the poloidal ducts. Quantitative analysis of the mass transfer processes associated with the tritium transport in the breeder as well as tritium diffusion through the structural and functional materials is important for two main reasons. The first is that there can be a substantial cost in extracting tritium from helium. The second is that tritium can make its way from the helium stream into the environment. In the present study, we analyze tritium transport in the front section of the DCLL DEMO-type Outboard blanket, where PbLi moves poloidally in a rectangular duct with an insulating flow channel insert (FCI) in the presence of a strong plasma-confining magnetic field. This involves two steps, the computation of the flow field with an MHD code, followed by the solution of the mass transfer equation with a newly-developed transport code CATRYS. The analyses included a sensitivity study to investigate how uncertainties in the properties of the materials (diffusion coefficient, solubility constant) affect the results and to assess the effect of an impervious crystalline sealing layer on the FCI.

I. INTRODUCTION

Tritium has a half life of about 12 years and is therefore scarce in nature. For this reason, proposed fusion reactors employing the D-T reaction will need to be self sufficient in tritium. This can be achieved by the use of lithium in the blanket surrounding the reactor chamber – tritium can be bred through the reaction of neutrons emanating from the plasma with lithium.

A number of blanket designs involve the use of lead-lithium (PbLi) flows, in which the PbLi flows through channels surrounding the chamber. One example is the Dual Coolant Lead Lithium (DCLL) blanket in which the PbLi serves as both a coolant and as a tritium breeder.

A proper understanding of the behavior of the PbLi flows and the production of tritium is vital to the design of the blankets, and the study of these systems is an active research area. A key consideration is that tritium diffuses

through steel walls, and it is necessary to minimize the losses to other parts of the plant or the environment. Extraction of tritium from the helium stream is expected to be costly, and licensing requirements will impose limits of the order of 1g/yr for losses to the atmosphere.

The approach taken here to the simulation of tritium transport is a two-step process. The first stage is to compute the flow field – in the blanket, there is a very strong magnetic field, and the flow is dominated by magnetohydrodynamic (MHD) effects. An established MHD/CFD solver, HIMAG (Refs. 1, 2), was therefore used for this task. The velocity field from HIMAG was then used as an input to a new code, CATRYS, which solves the equations for the transport of tritium. This approach is similar to that for the heat transfer analysis for the same DCLL blanket suggested earlier.³

The following sections discuss the computational approach in more depth, and present results obtained for flows through a DCLL duct. There is considerable uncertainty in the values for physical properties (e.g. solubility, diffusion coefficients) of materials used in these systems, and a key part of this work was to examine how these values would affect the results.

II. APPROACH TAKEN

As previously mentioned, the HIMAG code was used to obtain the flow field in a blanket channel. This code solves the equations for MHD flow using a finite volume method on an unstructured three dimensional grid.

For components that are present as a dissolved species, the transport can be modelled through the use of an advection/diffusion type equation. If trap sites and source terms are considered, the equation for the concentration of a species s , C_s , can be expressed as:⁴

$$\frac{\partial C_s}{\partial t} + \nabla \cdot J_s = S_s - \sum_k \left(\frac{\partial C_s^{t_k}}{\partial t} + v_s C_s^{t_k} \right) - v_s C_s + \sum_m v_m^s \left(C_m + \sum_k C_m^{t_k} \right) + S \quad (1)$$

where S is a source term the flux on the left hand side is given by $J_s = C_s \mathbf{u} - D_s \left(\nabla C_s + \frac{Q_s^* C_s}{kT^2} \nabla T \right)$.

The thermophoresis constant is Q_s^* , D is the diffusion coefficient, \mathbf{u} is the advection speed, and ν is the radioactive decay rate. The superscript t represents trapped atoms, k denotes different kinds of trap sites, and m represents parent nuclei of s . Traps result from irregularities in the structure, and are not relevant to the liquid phase. In the present study, the fluxes associated with the temperature gradients are assumed to be much smaller compared to those due to concentration gradients and thus were not included. These equations are supplemented by a set of boundary conditions expressing species flux and chemical potential balance at material interfaces. To ensure continuous flux we write:

$$D_L \frac{\partial C_s}{\partial n} \Big|_L = D_R \frac{\partial C_s}{\partial n} \Big|_R$$

If we assume that Sievert’s law holds, we can realise the second condition by imposing continuity of partial pressures:

$$\frac{K_L}{C_L} = \frac{K_R}{C_R}$$

The K coefficients are related to the solubilities, and L and R represent values on each side of the interface. Note that if the solubilities are different, the concentration will undergo a discontinuous change at the material interface.

Equation 1 and the closure relations required were incorporated into a new code, CATRYS, and were solved on a finite volume grid using a Crank–Nicholson scheme with the option of parallel computation. The velocity field was imported from the output of HIMAG, and interpolated onto the grid used by CATRYS.

III. SIMULATIONS AND RESULTS

The problem chosen for this work was the flow of PbLi through a front channel of a DCLL blanket with the flow channel insert and a cross section is shown in Fig. 1. The duct size, flow parameters, temperatures etc., relevant to the US DCLL DEMO blanket conditions, can be found elsewhere.^{3,5} The outer wall of the channel is constructed from reduced activation ferritic steel (RAFS) and just inside there is a flow channel insert of silicon carbide (SiC) composite with a 2mm gap in between. Some designs include pressure equalisation slots or holes in the FCI, but the present study considered a continuous FCI.

The present analysis considers a case with a mean flow velocity of 0.065ms^{-1} and an imposed magnetic field of 4T in the z direction, with a Hartmann number of about

15 000. Only the 2m section lying along the poloidal direction was considered and assumptions made were:

- the flow field is fully developed with the velocity everywhere parallel to the duct axis
- physical properties of the materials were constant
- concentration of tritium at the inlet is zero
- the mass transfer rate at the steel/helium interface is high relative to diffusion transport

The first of these may have some impact on the overall results; for example examination of the fully 3-D case⁶ reveals some counter flow (pressure equalisation slots can also lead to counter flow), and effects from the bends and end sections will not be accounted for. However, use of a fully developed profile does enable results to be generated fairly quickly. Moreover, as shown below, tritium permeation occurs mostly from the thin gaps, such that the above mentioned 3D effects in the bulk flow on the tritium permeation are not so important.

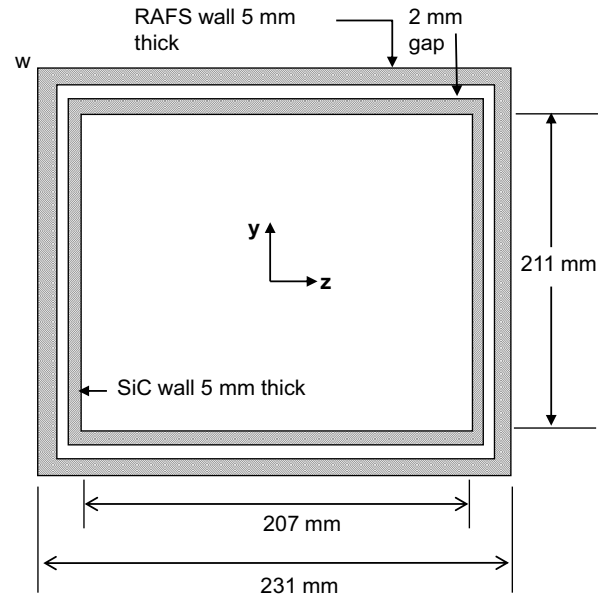


Fig. 1. Cross section showing DCLL geometry.

Variations in the solubilities and diffusion coefficients with temperature do occur, but since these variations are generally less than other uncertainties, it was considered that constant values would suffice.

The simulation presented here considered the front duct. This is the one the liquid enters first so the assumption of zero concentration at the inlet is probably reasonable. However, designs normally involve the liquid flowing through other ducts located behind the first one. Simulations of these sections would proceed in a similar manner, but with different inlet boundary conditions.

At the steel/helium interface, the transfer of tritium into the gas involves the recombination of tritium atoms into molecules, and the finite rate at which this takes place may influence the overall transport rate. Although the computational framework permits the incorporation of a recombination model, data for steel were not readily available, so this effect was not included.

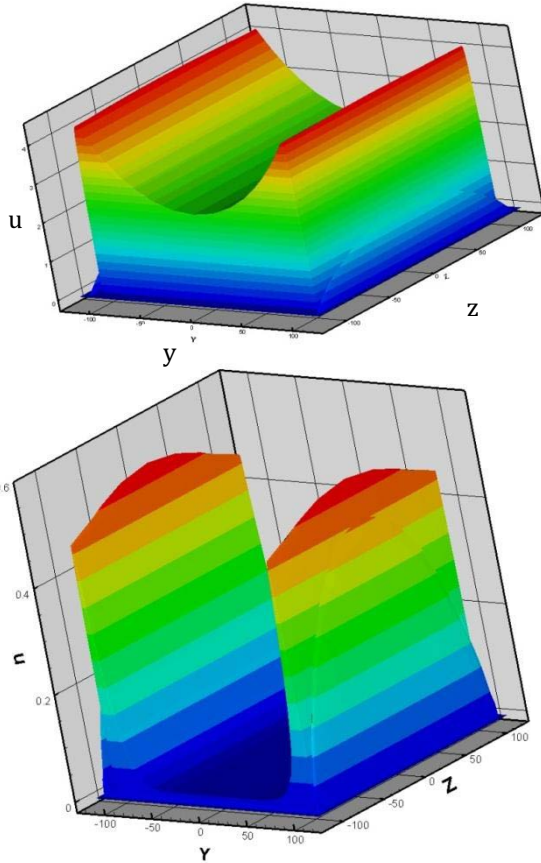


Fig. 2. Velocity profile across DCLL duct. Conductivity of FCI is $5 \Omega^{-1}m^{-1}$ (top) and $500 \Omega^{-1}m^{-1}$ (bottom).

The velocity field was obtained by performing a 2-D simulation of pressure gradient driven flow through the duct using HIMAG. A grid of 71×71 cells was used, clustered to provide higher resolution in the near wall regions; the gaps were spanned by 6 cells. The parameters chosen for the electrical conductivities were $\sigma_{PbLi} = 7 \times 10^5 \Omega^{-1}m^{-1}$, $\sigma_{Steel} = 1.46 \times 10^6 \Omega^{-1}m^{-1}$ and for the FCI, values from $\sigma_{SiC} = 5 \Omega^{-1}m^{-1}$ to $500 \Omega^{-1}m^{-1}$ were used. The dynamic viscosity of the fluid was taken to be $10^{-3} \text{ kg m}^{-1}s^{-2}$. The simulations were run until convergence, and plots showing the velocity field for the cases with the highest and lowest FCI conductivities used are shown in Fig. 2. The profiles are characterised by relatively high velocities near the walls parallel to the applied magnetic field with lower velocities toward the centre. An important feature is that in the gaps

perpendicular to the field the velocities are very low, particularly for low FCI conductivities. This cannot be seen easily in these figures, but other plots can be found elsewhere.^{3,7} These findings confirm earlier observations for various FCI flows.⁷

For the mass transport calculation, a 3D grid with 50 cells in the streamwise direction was used. In the other directions, a slightly coarser mesh was used. Consideration of the length and time scales for diffusion shows that the resolution requirements for mass transport computations are less demanding than for MHD simulations for the diffusion coefficients used in this study. The velocity field was taken from the 2-D computation and scaled so as to give a mean velocity of 0.065 ms^{-1} . The tritium mass generation rate was computed as $S_T = 4.9 \times 10^{-9} \exp(-3.0y)$ where y is the distance from the front of the unit.

There is considerable uncertainty in the diffusion and solubility coefficients of tritium in PbLi⁸, and a set of simulations was performed with different values, covering the range found in the literature. Diffusion coefficients for SiC vary by several orders of magnitude depending on whether it is amorphous or crystalline – at present, it appears that manufacture of FCIs with a crystalline sealing layer on either SiC composite or foam is feasible; since this would be preferred due to its very low electrical conductivity a low value of D was used ($5 \times 10^{-16} \text{ S m}^{-1}$).

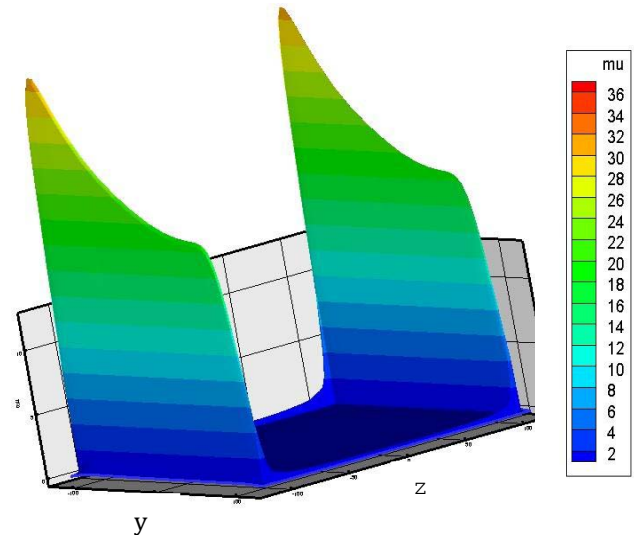


Fig. 3 Concentrations ($10^{-6} \text{ kg m}^{-3}$) at 1.5m from inlet for solubility of $0.05 \text{ mol m}^{-3} \text{ Pa}^{-1/2}$; $\sigma_{FCI} = 5 \text{ S m}^{-1}$ and $\sigma_{PbLi} = 7 \times 10^5 \text{ S m}^{-1}$

Figure 3 shows the concentration profile at a cross section located 1.5 m from the inlet. The concentrations in those parts of the gap aligned perpendicular to the field are considerably higher than other parts of the duct, and are associated with very low fluid velocities. One finding was that for cases with very low solubility, the

concentrations in the gap levelled off with distance from the inlet, indicating that the loss of tritium through the walls is roughly equal to the generation rate. This can be attributed to the high partial pressure associated with the low solubilities, which leads to a high loss rate. This effect is shown quantitatively in Fig. 4, which shows the mass of tritium per unit length (i.e. the concentration integrated over the area) for two different solubilities.

The effect of solubility on the concentration can also be seen in Fig. 5, which shows the concentrations along lines perpendicular to the duct axis at $x=1.5\text{m}$ for both $y=0$ and $z=0$. Note the step change in the concentration at the steel/liquid interface; the concentration ratio is equal to the solubility ratio. In Case 1, which has a low solubility for the liquid, this means that a high concentration gradient can be maintained in the steel for a given liquid concentration. Case 2 has a much higher solubility, which results in a very low gradient on the steel side, and consequently a much lower leakage rate.

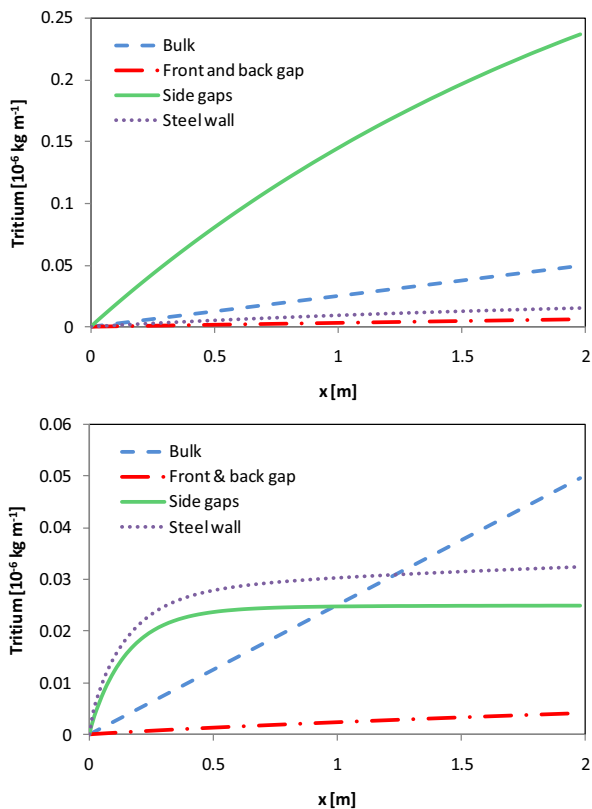


Fig. 4 Mass of tritium per unit length $S=0.05 \text{ mol m}^{-3} \text{ Pa}^{-1/2}$ (top) ; $S=0.001 \text{ mol m}^{-3} \text{ Pa}^{-1/2}$ (bottom) ; $\sigma_{\text{FCI}} = 5 \text{ S m}^{-1}$. In this geometry, the side gaps are the Hartmann gaps.

In order to more clearly see how the different properties affect the leakage of tritium from a DCLL module, variation of the loss rates with each property was

examined more closely. The reference case selected for this study used the following values for the diffusion and solubility coefficients of T in PbLi, $D = 2.54 \times 10^{-9} \text{ m}^2 \text{ s}^{-1}$, $S = 0.01 \text{ mol m}^{-3} \text{ Pa}^{-1/2}$ and $\sigma = 5 \text{ S m}^{-1}$. The values that were used for the ferritic steel were $D = 1.5 \times 10^{-8} \text{ m}^2 \text{ s}^{-1}$ and $S = 0.0025 \text{ mol m}^{-3} \text{ Pa}^{-1/2}$ (Refs 8, 9).

These represent best estimates of these quantities and are roughly in the middle of the range of values available. Note that while the transport is not *directly* dependent on the electrical conductivity of the FCI, the flow field depends strongly on this property and so will influence the tritium transport.

Figure 6 shows the losses as each parameter is varied while the others remain at the reference values. The entire tritium production rate in the unit was calculated to be $3400 \times 10^{-12} \text{ kg s}^{-1}$ so the maximum total loss is about 2%. In this set of results, the diffusion coefficient in the FCI had been assumed to be very low, which is likely to be a reasonable assumption if the SiC has a crystalline layer.

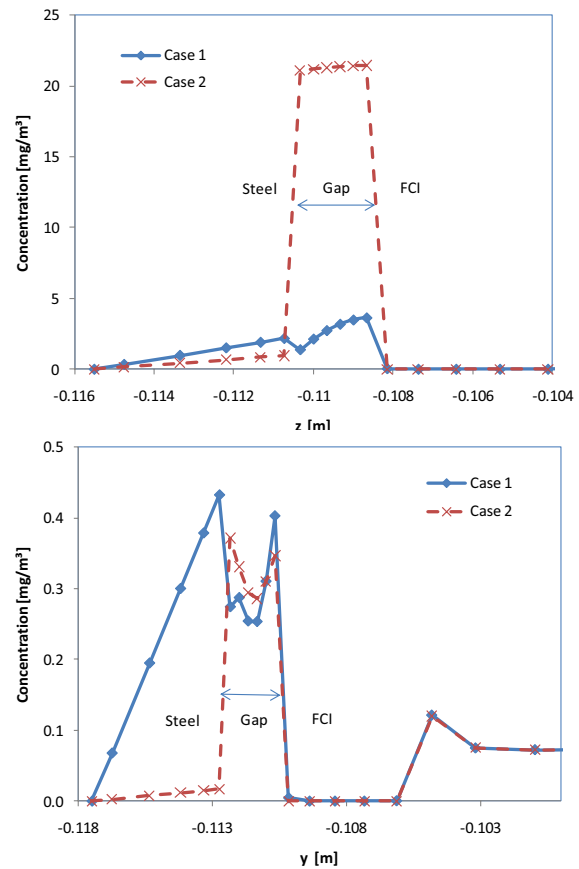


Fig. 5. Concentration profiles at $x=1.5\text{m}$, $y=0$ (top) and $z=0$ (bottom). For Case 1, $D=2.54 \times 10^{-9} \text{ m}^2 \text{ s}^{-1}$ and $S=0.001 \text{ mol m}^{-3} \text{ Pa}^{-1/2}$; for Case 2, $D=7 \times 10^{-9} \text{ m}^2 \text{ s}^{-1}$ and $S=0.05 \text{ mol m}^{-3} \text{ Pa}^{-1/2}$

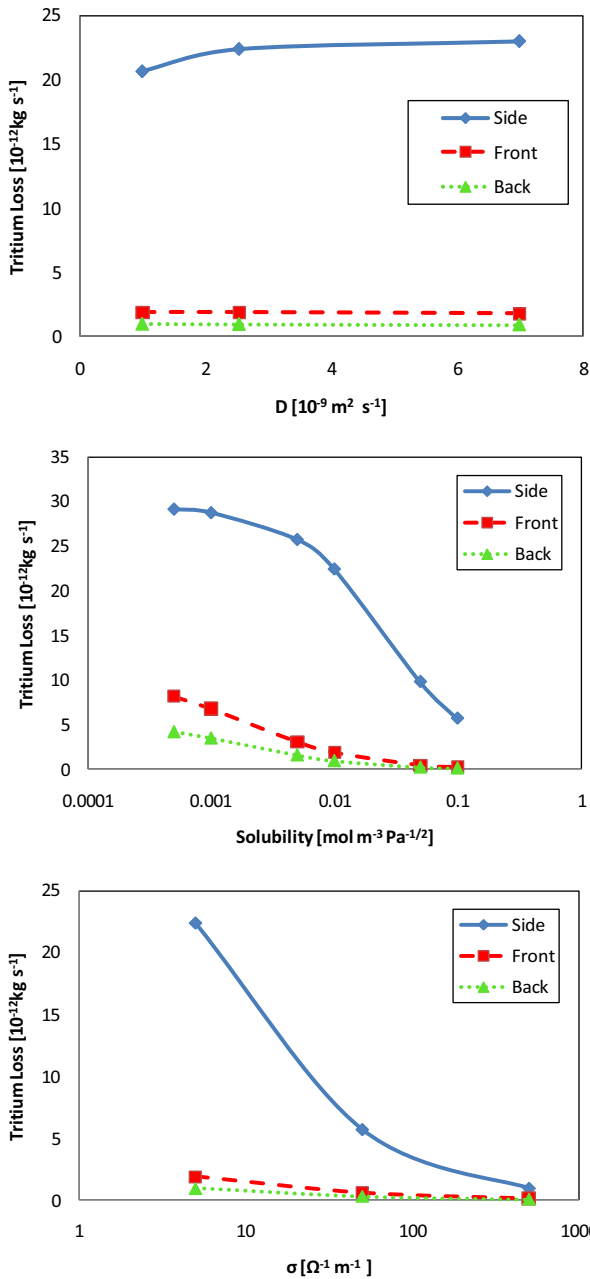


Fig. 6. Tritium loss rate as a function of diffusion coefficient and solubility of the PbLi, and FCI conductivity.

IV. CONCLUSIONS

The transport of tritium in the front unit of a DCLL US DEMO blanket has been investigated numerically. The main losses arise from the presence of very slow moving fluid in the Hartmann gaps between the FCI and the RAFS wall, while the tritium generated in the bulk flow inside the FCI remains there. There is considerable uncertainty in several properties which influence tritium

transport, but although the data for solubility in PbLi vary by two or three orders of magnitude, the corresponding variation in the loss rate is only about 5. The SiC FCI with a crystalline sealing layer can be considered as a tritium permeation barrier, such that the maximum amount of tritium permeated into helium streams is as much as 2% of the total tritium production.

ACKNOWLEDGMENTS

The development of the MHD models and code was funded by the US Department of Energy (DOE) under grant No. DE-SC-0002380.

REFERENCES

1. M.-J. NI, R. MUNIPALLI, P. Y. HUANG, N. B. MORLEY and M. A. ABDU, "A current density conservative scheme for incompressible MHD flows at a low magnetic Reynolds number. Parts 1 and 2," *J. Comp. Phys.*, **227**, 174 (2007).
2. N. B. MORLEY, M.-J. NI, R. MUNIPALLI, P. Y. HUANG, and M. A. ABDU, "MHD simulations of liquid metal flow through a toroidally oriented manifold," *Fusion Eng. and Des.*, **83**, 1335 (2008).
3. S. SMOLENTSEV, M. ABDU, N. B. MORLEY, M. SAWAN, S. MALANG, C. WONG, "Numerical analysis of MHD flow and heat transfer in a poloidal channel of the DCLL blanket with a SiCf/SiC FCI," *Fusion Eng. and Des.*, **81**, 549-553 (2006).
4. G. R. LONGHURST, "Verification and validation of TMAP7 User manual," INEEL/EXT-04-02352 Rev. 2, Idaho National Lab (2008).
5. C. P. C. WONG et al., "An overview of dual coolant Pb-17Li breeder first wall and blanket concept development for the US ITER-TBM design," *Fusion Eng. and Des.*, **81**, 461-467 (2006).
6. N. B. MORLEY, M.-J. NI, R. MUNIPALLI, P. HUANG and M. A. ABDU, "MHD simulations of liquid metal flow through a toroidally oriented manifold," *Fusion Eng. and Des.*, **83**, 1335-1339. (2008).
7. S. SMOLENTSEV, N. B. MORLEY, M. ABDU, "MHD and thermal issues of the SiCf/SiC flow channel insert," *Fusion Sci. Tech.*, **50**, 107-119 (2006).
8. E. MAS DE LAS VALLS, L. A. SEDANO, L. BATET, I. RICAPITO, A. AIELLO, O. GASTALDI and F. GABRIEL, "Lead-lithium eutectic material database for nuclear fusion technology," *J. Nuc. Mat.* **376**, 353 (2008).
9. A. AIELLO, A. CIAMPICHETTI, G. BENAMATI, "Hydrogen permeability and embrittlement in Eurofer 97 martensitic steel," ENEA Report SM-A-R-001 (2003).